

Hydrolysis and Other Phenomena Affecting Structure and Performance of Polyamide 6 Membrane

C. W. YAO, R. P. BURFORD,* A. G. FANE, C. J. D. FELL, and R. M. McDONOGH, *School of Chemical Engineering and Industrial Chemistry, The University of New South Wales, Kensington, NSW 2033, Australia*

Synopsis

The rate of hydrolysis of polyamide 6 in membrane casting solution containing strong mineral acid has been studied by determining changes in molecular weight, as estimated from dilute solution viscometry measurements. Hydrolysis is shown to be first order with a long half-life of about 250 days. A two-step dissolution process for polyamide 6 is proposed. The effect of extended dope maturation time upon polyamide 6 membrane preparation and performance has been examined. At short maturation times where protonation of polymer chain is occurring, flux is relatively low. A major increase in flux occurs after about 10 h, when protonation appear complete and hydrolysis has begun. Hydrolysis reduces polymer chain entanglement, and so quite different mechanisms for membrane formation exist as dope maturation time proceeds. With chains less than the critical entanglement length, nodular top layer membranes and alveolar walls lead to high water flux. However, such membranes are quite fragile.

INTRODUCTION

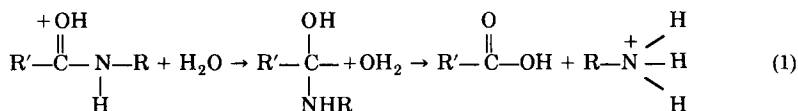
A novel ultrafiltration membrane produced from aliphatic polyamides using low-cost protic (acid) solvent was first described in 1978.¹ The potential applications of these membranes have been discussed.² In a recent paper³ we have reported how the structure and performance of the polyamide membrane varies with polymer/solvent ratio in the casting solution (dope). These dopes were prepared using relatively short dope maturation times (< 3 h). For such short maturation times the "dissolution" involved formation of a colloidal dispersion of aggregated polymer chains with little hydrolytic scission of the polymer backbone.⁴ However, it is known^{5,6} that polyamides are gradually hydrolyzed in strongly acidic environments so that long maturation dopes would be expected to differ from short maturation dopes, and result in different membrane structure and performance. In this paper we report on hydrolysis and molecular weight change in long maturation dopes and on the properties of the resultant membranes.

Hydrolysis

In concentrated sulphuric acid, simple secondary amides hydrolyse either unimolecularly ($A - 1$)⁵ or bimolecularly ($A - 2$),⁶ the latter predominating

*To whom correspondence should be addressed.

where water is available (in this case at acid concentrations below 78%). The A - 1 mechanism involves a slow heterolytic cleavage of the protonated amide resonance form. For bimolecular hydrolysis (A - 2), slow hydration of the protonated amide occurs at the carboxyl group, followed by fast cleavage:



A typical protic solvent used for polyamide dope is 6*M* HCl,¹⁻³ where water is abundant and it can be assumed that the bimolecular hydrolysis mechanism will predominate. While mechanistic studies of the hydrolysis of polyamides have not identified the nature of the original protonation step, the fact that hydrolysis is first order in sulfuric acid at various temperatures is well established.⁷⁻¹⁰ Most researchers use end-group and viscosity methods to monitor changes in molecular weight, but the analysis by Hoshino and Watanabe⁷ appears to be the most rigorous.

Here the degree of depolymerization according to the Montroll parameter⁷ α can be related to changes in intrinsic viscosity by

$$\frac{[\eta]_t}{[\eta]_0} = \left\{ \frac{\ln p}{\ln [p(1 - \alpha)]} \right\}^{1/\alpha} \quad (2)$$

where α is the Mark-Houwink-Skurada constant for the appropriate polyamide/solvent pair and p is the extent of reaction. The degree of depolymerization can then be related to a degradation constant λ , by

$$\lambda = - \left[\ln \frac{(1 - \alpha)}{t} \right] \quad (3)$$

and thus the half-life of the polymer can be determined. In our present study we wish to monitor molecular weight changes of highly concentrated solutions of polyamide 6 in hydrochloric acid, for which the half-life has not been previously documented.

Membrane Structure and Performance

The second important aim is to discover how such hydrolysis affects polyamide membrane properties. To date, the main work relating molecular weight to membrane structure and performance has been restricted to ethylene-vinyl alcohol copolymers.¹¹ Higher molecular weight led to small pores and low water fluxes, while lower molecular weight gave a higher pore density. Thus higher water fluxes were found, even though pore size remained small. In this work, no hydrolytic studies were undertaken (the solvent was aqueous isopropanol) with various molecular weight fractions of the polymer being obtained by bulk fractional precipitation prior to preparation.

According to the coagulation mechanism suggested by Matsumoto et al.,¹¹ the lower molecular weight fractions were below the critical value required for

entanglement, with discrete fragments in free association. For molecular weights above 40,000 Daltons (as determined by GPC) high intermolecular entanglement existed as open fringed micelles, and this structure was assumed to persist during membrane formation, leading to large but closed cells. This contrasts with the aggregates formed from short polymer chains, which associate to give small but open cells. Their results suggest that they studied membranes produced with molecular weight fractions ranging from below the critical entanglement molecular weight to well beyond this value.

The state of molecular aggregation of polymers in varying solvents which may affect gelation of polyacrylonitrile, poly(vinyl alcohol), and gelatin has been hypothesized by Labudzinska and Ziabicki.¹² These highly concentrated polymer solutions slowly form interpenetrating networks which have increased viscosities. This phenomenon is conceptually the inverse of dope maturation, where entanglements are likely to decrease with ageing time. The molecular mechanism of gelation associated with phase inversion may be applicable to the membrane coagulation step. For shorter chains, a heterogeneous network like that of Matsumoto is proposed, but for longer chains a relatively homogeneous network is described.

In dilute nonassociating solutions, viscosity decreases as a simple function of decreasing polymer molecular weight. However, in concentrated membrane dope where solvents are highly protic and in which polymer aggregation is important, viscosity changes will also reflect varying aggregate association. Thus different membrane structure can be obtained, depending upon the applicable coagulation mechanism. This could be quite pronounced if the polyamides under investigation in this work suffer sufficient hydrolysis to cause the polymer to be below the critical molecular weight.

EXPERIMENTAL

Dope Preparation

The same dope formulation was employed throughout and comprised a quaternary mixture of polyamide 6 yarn ("Tedjin") of 20 denier (25.5% by weight), 10*M* hydrochloric acid (49.1% by weight), water (21.2% by weight), and ethyl alcohol (4.2% by weight) mixed at 20°C. A "master batch" of dope was prepared in sufficient quantity to enable aliquots to be withdrawn at various maturation times for molecular weight determination and concurrent membrane preparation.

Intrinsic Viscosity Measurement

The technique involved stopping the maturation/hydrolysis process at a given time by casting a membrane, and then dissolving this in a nonhydrolyzing solvent prior to viscosity measurements. Membranes were prepared from about 5 g of aged dope in an excess of water at 20°C. After retrieval, about 1 g of membrane was dried at 60°C for 15 h, to give a white opaque film of constant weight. Four solutions were prepared in 85% aqueous formic acid at $25 \pm 1^\circ\text{C}$ over the concentration range 0.78–0.26 g/dL. Mean flow times were drawn from five Ubbelohde viscometer measurements, and were used to obtain η_{sp} , from which the intrinsic viscosity $[\eta]$ was obtained in the usual

way. Duplicate dope coagulations were performed, from which $[\eta]$ was found to vary by no more than 1%. Molecular weight was then determined using the semiempirical equation¹³

$$\bar{M}_n = 13,000[\eta]^{1.39}$$

Scanning Electron Microscope Studies

Membrane structure was examined with a Cambridge Stereoscan S4-10 scanning electron microscope. Air-dried samples were prepared for skin and bottom surface examination. Cross sections of the membranes were first embedded in standard grade "Spurr" epoxy resin and then sectioned with a Riechert-Jung Ultracut microtome using a glass knife. All samples were etched in a saturated NaOH/ethanol solution for 0.5 h before they coated with gold using a "Polaron" sputter coater with magnetron head. The Robinson backscatter detector was employed to reduce charging.

Cloud Point Determination

Dilute solutions of 0.5, 1, 2, 3, 5, 7, 10, and 13% w/w of polyamide 6 in 10M HCl were prepared. The nonsolvent, i.e., water, was slowly added to these solutions. Permanent turbidity was detected visually, and the composition of the solution at the cloud point was calculated from the fraction of the total amounts in solution present.

Water Permeability Measurement

Membrane permeability was measured with distilled water in a 150 mL capacity bath cell with 16 cm² membrane area, at a pressure of 100 kPa and a temperature of 20°C. Water flux was allowed to stabilize over a period of 0.5 h and then monitored over a 1 h period. Data are reported as liters per square meter per hour.

RESULTS AND DISCUSSION

Molecular Weight Changes

The change in apparent molecular weight with dope maturation time is summarized in Figure 1. The unaged polymer molecular weight increased initially from 10,500 to a maximum of about 12–13,000. This could be attributed to the formation of protonated polymer/counterion complex. We see a net weight increase of about 24%, while for stoichiometric polymer-acid complexing without hydrolysis a maximum weight increase of about 31% is possible. The protonation step is common to both A - 1 and A - 2 mechanisms. This is rapid (as reflected by an observed step increase in pH³), and by reducing interpolymer hydrogen bonding a relatively low dope viscosity at high polymer concentrations is possible. This first dissolution step is mentioned for polyamides by Epstein and Rosenthal,¹⁴ where a 1.02 mol HCl gas/mol —CONH— "titration" result was found. High surface area yarns allow ready access of solvent to polymer, even though diffusion rates through the crystalline solid will be low.

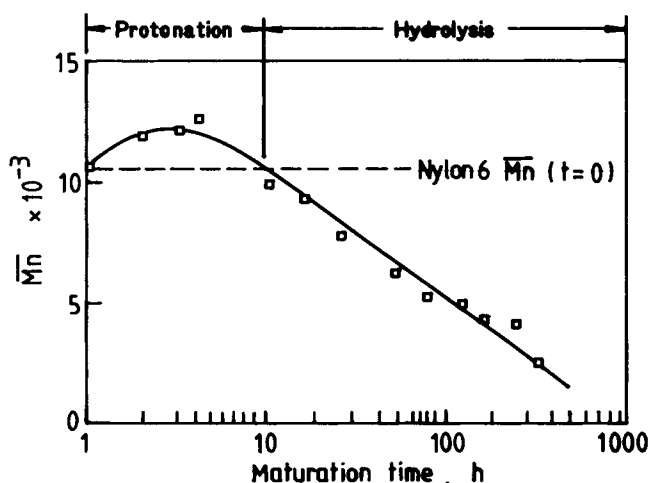


Fig. 1. Average number molecular weight vs. dope maturation time.

The polymer-solvent complex thus formed now slowly hydrolyzes, as shown by the linear portion of the graph. This appears constant at ageing times greater than 10 h, with rate constants being given in Table I at various maturation times.

The approximately constant values of λ confirm that the first-order kinetic equation (3) cited previously is valid, and is consistent with the kinetic findings for polyamides in other acids. The hydrolysis half-life is defined as the time required for half of all amide bonds to be cleaved, and will be $(\ln 2/\lambda)$. For our solution, the half-life is about 250 days. While this might appear to be a lengthy time, it is also quite apparent from Figure 1 that molecular weight is noticeably reduced over quite short maturation periods. If the concepts of Matsumoto et al.¹¹ and others¹² are valid, polyamide 6 molecular weight may quickly fall below a nominal critical entanglement molecular weight of about 10^4 . For example, after about 72 h dope maturation

TABLE I
Rate Constant of Hydrolysis in the Dope

Dope maturation time (h)	$[\eta]_{25^\circ\text{C}}$	$1 - \alpha$	$\lambda \times 10^4$ (h^{-1})
0	0.86	1.0000	—
10	0.82	0.9994	0.5
16	0.79	0.9986	0.8
24	0.70	0.9964	1.5
48	0.60	0.9927	1.5
72	0.52	0.9890	1.5
120	0.50	0.9875	1.0
168	0.45	0.9846	0.9
238	0.40	0.9789	0.9
336	0.30	0.9660	1.0
Average			1.0

time, we found that membranes were quite brittle and fragile. This is evidence that polymer molecular weight has fallen below the critical value.

Membrane Performance and Morphology

The water fluxes at different maturation times are given in Table II. It can be seen that at short times, where hydrolysis is minimal but protonation has occurred, flux values are low. Here, one can surmise that polymer molecular weight is sufficiently high for entanglement so that some association or alignment of chains persists at the time of phase inversion. Thus, some continuity in cell wall structure will exist, resulting in a membrane having a cross section comprising predominately closed cells.

The best established theories for skin formation rationalize the process as being physical gelation.¹⁵⁻¹⁷ This proceeds either by molecular aggregation¹¹ with small chains fibrils protruding from the highly swollen core [as represented by low molecular weight in the dope model in Fig. 2(d)] or by *in situ* overlapping of much longer entangled polymer chains from a less swollen core [high molecular weight polymers in the dope in Fig. 2(a)].

We propose that commercial polyamide fibers contain chains considerably longer than the critical entanglement length. At short dope maturation times, sufficiently long fibrils can extend from the swollen core of fibers (colloids) to cause entanglement or alignment. With longer dope maturation times the protruding, partially solvated fibrils will hydrolyze, leading to shorter segments unable to align and entangle. Ultimately, the colloidal aggregate will completely disperse leaving a solution of short fully dissolved segments. However, this is well beyond the time scale of our observations, since even at 72 h maturation the dope was turbid, indicating a colloidal suspension. Changes in membrane structure and performance over relative short aging times but at elevated temperatures have been reported by us elsewhere.^{3,18}

As membranes form from the short maturation time dopes (i.e., the protonation stage dopes), a homogenous solid polymer layer rapidly overlaps by infinite network gelation of the entangled fibrils. The interior of swollen core fibrils (colloids) precipitates slowly because of retarded water diffusion. As the colloid precipitates more slowly than the entangled fibrils, interfacial stresses develop, leading to voids.

The mechanism for this step is based on Strathmann's model¹⁹ and involves the translocation of unsolidified colloid particles below the solidified (gelled)

TABLE II
Influence of Maturation Time on Water Fluxes

Dope maturation time (h)	Water flux $1/m^2$ (h)	\bar{M}_n
1	150	10,700
4	170	12,600
10	1150	9,900
16	1380	9,300
24	2170	7,800
48	2970	6,300

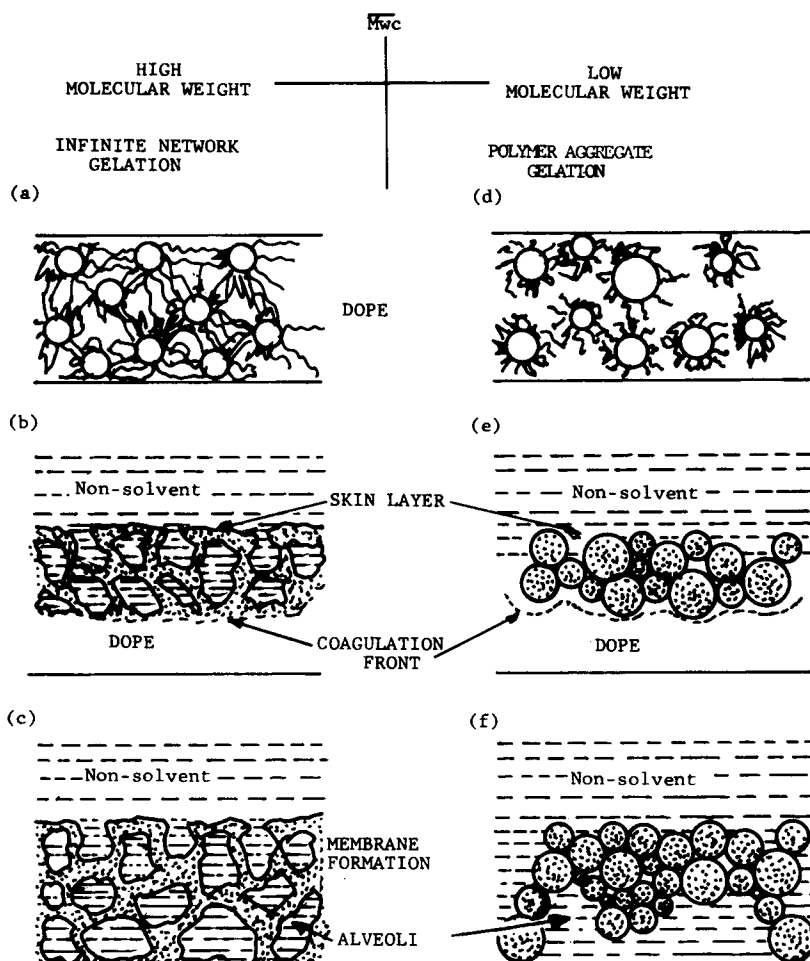


Fig. 2. Schematic diagram of the influence of gelation mechanism upon the coagulation process in membrane formation.

entangled layer brought about by the osmotic flow of nonsolvent (water) into the underlying dope, together with associated shrinkage stress. The result of this is surface pores as represented by Figure 2(b). These pores can be seen at varying maturation times on the top layer of membranes in Figure 3. It should be noted that the 4 h matured sample has a matrix which is essentially homogeneous, reflecting the entangled fiber structure prior to precipitation, whereas at longer maturation times the solid matrix is much more irregular and nodular in appearance. This is illustrated by comparing Figures 2(b) and 2(e). The surface pores seen in Figure 3 after 10 and 72 h maturation are thought to represent defects in packing, or aggregation, of swollen but poorly linked colloids.

The cross-sectional development continues to reflect the two mechanisms. Where molecular weight is high and entanglement persists, an alveolar structure in which the walls are more or less continuous is generated. This *P*-type structure²⁰ is represented by Figure 2(c) and is shown microscopically in

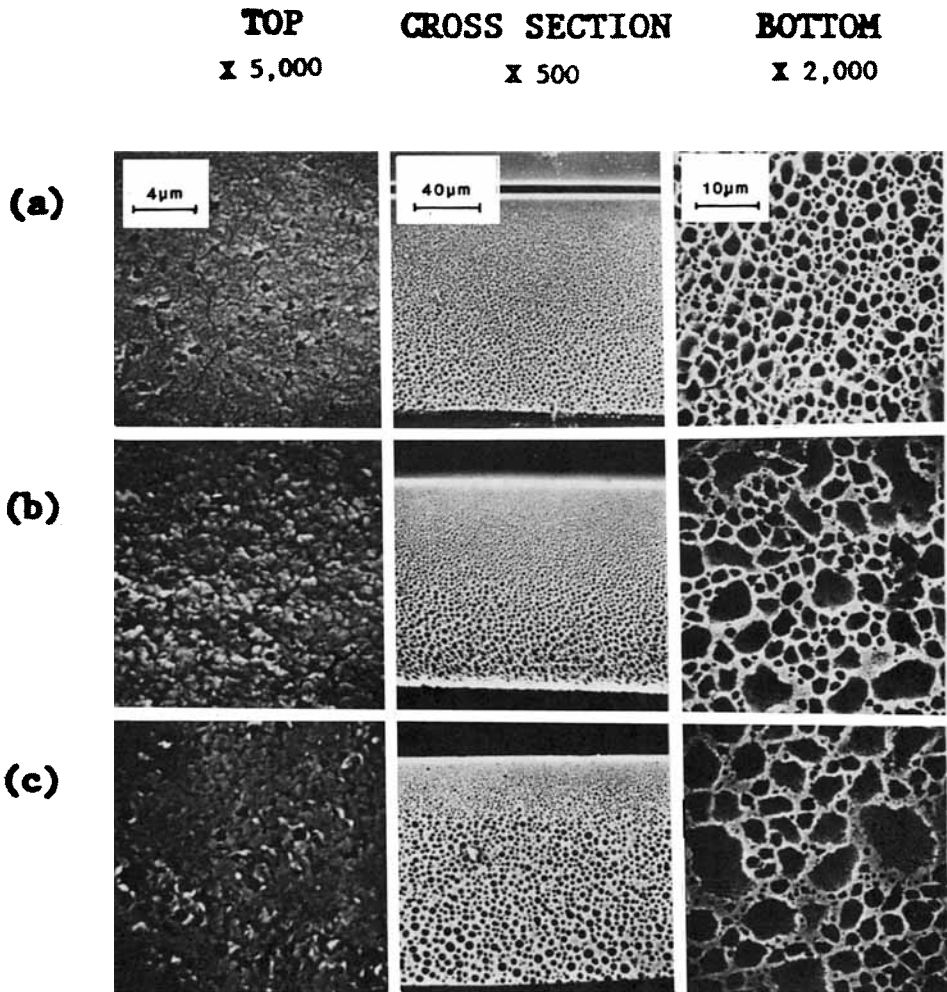


Fig. 3. Scanning electron micrograph of membrane structure with different maturation times (h) of the dope: (a) 4; (b) 10; (c) 72.

Figure 3(a). The bottom layer shows alveolar wall homogeneity, which would provide resistance to water flow. The relatively low water flux values shown in Table II are consistent with this structure.

For dopes of longer maturation times the swollen "colloidal" entities are smaller and have shorter fibrils, and on phase inversion these colloids forming heterogeneous and porous alveolar walls (O-type²⁰). This is represented by Figure 2(f) and shown by the SEM views in Figures 3(b) and 3(c). The mosaic-like texture revealed by the bottom surface in particular provides an explanation for the very high water fluxes found at longer maturation times (Table II).

Inspection of the cross sections in Figure 3 shows that the long maturation dopes produce a more asymmetric structure. This may be because these dopes require more nonsolvent before phase inversion occurs, and this makes the structure more sensitive to concentration gradients of nonsolvent during

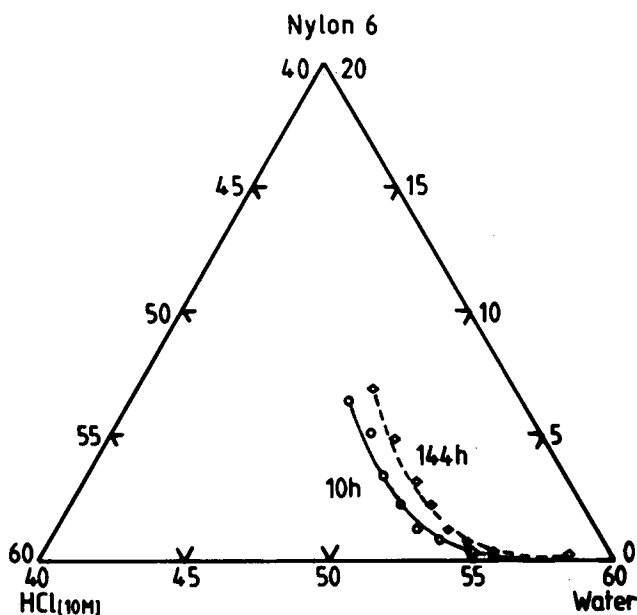


Fig. 4. Phase diagram for polyamide 6/HCl/water system showing the cloud point curve determined by titration, as a function of dope maturation time (h): (a) 10; (b) 144.

formation. Evidence is provided in Figure 4 which shows the cloudpoint curve at 10 h, curve (a) shifts towards the nonsolvent after 144 h, curve (b).

The dramatic changes in water flux and associated changes in membrane morphology arising from hydrolysis over extended maturation times complements our previous study reported over a much shorter ageing period.^{3,18} In that case, while changes in polymer concentrations, acid strength, temperatures, etc., were investigated, the time frame was confined to the protonation stage.

APPENDIX: NOMENCLATURE

a	exponential parameter in Mark-Houwink-Skurada equation; a measurement of solvent-polymer interaction
\overline{M}_n	average number of molecular weight
\overline{M}_{wc}	critical weight average molecular weight for polymer entanglement
p	the extent of reaction
t	dope maturation time (h)
α	degree of depolymerization in Montroll equation
λ	degradation constant or hydrolysis rate constant (h^{-1})
$[\eta]_0$	intrinsic viscosity before hydrolysis
$[\eta]_t$	intrinsic viscosity after hydrolysis at time t
η_{sp}	specific viscosity

References

1. M. S. Lefebvre and C. J. D. Fell, Australian pat. application 40897/78 (1978).
2. M. S. Lefebvre, C. J. D. Fell, A. G. Fane, and A. G. Waters, in *Ultrafiltration Membrane and Application*, R. Cooper, Ed., Plenum, New York, 1980, p. 79.

3. R. M. McDonogh, A. G. Fane, and C. J. D. Fell, *J. Membr. Sci.*, **31**, 321 (1987).
4. K. Hoshino, *Chem. Soc. Jpn. Bull.*, **19**, 156 (1944).
5. V. K. Krieble and K. A. Holst, *J. Am. Chem. Soc.*, **60**, 2976 (1938).
6. J. A. Duffy and J. A. Leisten, *J. Chem. Soc.*, **1960**, 853.
7. K. Hoshino and M. Watanabe, *J. Am. Chem. Soc.*, **73**, 4816 (1951).
8. A. Pakshver and E. Mankash, *Colloid J. USSR*, **14**, 125 (1952).
9. P. J. Flory, *Chem. Rev.*, **39**, 137 (1946).
10. E. F. Cassasa, *J. Polym. Sci.*, **4**, 405 (1949).
11. T. Matsumoto, K. Nakamae, T. Ochiuni, and S. Horie, *J. Membr. Sci.*, **9**, 109 (1981).
12. A. Labudzinska and A. Ziabicki, *Kolloid Z. Z. Polym.*, **243**, 21 (1971).
13. G. B. Taylor, *J. Am. Chem. Soc.*, **69**, 635 (1947).
14. M. E. Epstein and A. J. Rosenthal, *Text. Res. J.*, **36**, 813 (1966).
15. J. G. Wijmans, J. P. B. Baaij, and C. A. Smolders, *J. Membr. Sci.*, **14**, 263 (1983).
16. M. H. V. Mulder, J. O. Hendrikman, J. G. Wijmans, and C. A. Smolders, *J. Appl. Polym. Sci.*, **30**, 2805 (1985).
17. A. J. Reuvers, F. W. Altena, and C. A. Smolders, *J. Polym. Sci., Part B: Polym. Phys.*, **24**, 793 (1986).
18. R. P. Burford, R. M. McDonogh, C. J. D. Fell, A. G. Fane, and C. W. Yao, in *Synthetic Polymeric Membranes*, B. Sedlacek, Ed., Walter de Gruyter, Berlin, New York, 1987, p. 149.
19. H. Strathmann, K. Kock, P. Amar, and R. W. Baker, *Desalination*, **16**, 179 (1975).
20. G. J. Gittens, P. A. Hitchcock, D. C. Sammon, and G. E. Wakley, *Desalination*, **8**, 369 (1970).

Received February 10, 1987

Accepted March 31, 1987